J. Indian Chem. Soc.,
Vol. 96, May 2019, pp. 577-583

Thermal behavior and decomposition mechanism of a series of crown ether based lanthanide(III) hexacyanometallate(III) compounds

Rajesh Koner*[a,b], Phalguni Misra[a] and Shuvankar Mandal[a]

[a]Department of Chemistry, University of Calcutta, Kolkata-700 009, India

[b]Department of Chemistry, Bhairab Ganguly College, Belghoria, Kolkata-700 056, India

E-mail: rkbgc2010@gmail.com

Manuscript received online 10 March 2019, revised 09 April 2019, accepted 10 April 2019

Thermal decomposition reactions of eight lanthanide(III) compounds (Ln = Ce, Nd, Sm, Eu, Gd and Tb) having l8-crown-6 and water molecules in the inner sphere and hexacyanoferrate(III)/hexacyanochromate(III)/hexacyanocobaltate(III) in the secondary sphere have been performed by means of TG-DTA in an atmosphere of dry nitrogen. The results show that the dissociation processes consist of several steps. The compositions of the products and the dissociation mechanisms have been understood from relative weight loss as well as from elemental analyses and FT-IR spectral data. It has been found that the relative stability with respect to the decomposition of the crown ether moiety depends on the atomic number of lanthanides or the nature of the 3d metal ion in the hexacyanometallate(III).

Keywords: Lanthanide(III), l8-crown-6, hexacyanometallate, TG-DTA, dissociation mechanism.

Introduction

Thermogravimetric analysis is a reliable method for studying physico-chemical behavior of coordination compounds[1,2]. There is a very close relation between thermogravimetric, calorimetric and spectroscopic data for coordination compounds[3]. Notably, there has been considerable interest in the lanthanide(III) compounds of crown ethers during the past several decades[4]. Although, the thermal behavior of several such compounds have been reported earlier[5,6], the decomposition mechanism has not been well investigated. Some of us reported previously the syntheses and characterization of a series of lanthanide(III) compounds having 18-crown-6 as a primary ligand and a hexacyanometallate as the counter anion[7,8]. The compositions of these reported systems are $[Ln^{III}(18\text{-crown-6})(H_2O)_4][Fe^{III}(CN)_6]\cdot 2H_2O$ (**1**: Ln = Ce; **2**: Ln = Nd) and $[Ln^{III}(18\text{-crown-6})(H_2O)_3][M^{III}(CN)_6]\cdot 2H_2O$ (**3**: Ln = Sm, M = Fe; **4**: Ln = Eu, M = Fe; **5**: Ln = Tb, M = Fe; **6**: Ln = Gd, M = Fe; **7**: Ln = Gd, M = Cr; **8**: Ln = Gd, M = Co). We anticipated that thermal degradation of this series of compounds would be interesting due to following reasons: (i) there are a number of coordinated and solvated water molecules; (ii) cyanide may be produced from a hexacyanometallate during heating, which in turn, may produce heterometallic cyanides without an organic ligand. Accordingly, we have performed TG-DTA of the above mentioned series of eight compounds. Herein, we report TG-DTA of **1**-**8**, elemental analyses and FT-IR spectral data of the products in various steps and dissociation mechanism.

Experimental

Materials and physical methods:

The compounds **1**-**8** were prepared according to the reported method[7,8]. Elemental (C, H and N) analyses were performed on a Perkin-Elmer 2400 II analyzer. Thermogravimetric and differential thermal analyses were performed on a Metler Instrument in an atmosphere of dry nitrogen at a heating rate of 2°C min^{-1} using an alumina crucible as the container. FT-IR spectra were recorded in the region 400–4000 cm^{-1} on a Bruker-Optics Alpha-T spectrophotometer with samples as KBr disks.

Results and discussion

Thermal analysis and decomposition mechanism of the compounds:

Combined thermogravimetric (TG) and differential thermal analysis (DTA) of $[Ln^{III}(18\text{-crown-6})(H_2O)_n][M^{III}(CN)_6]\cdot$

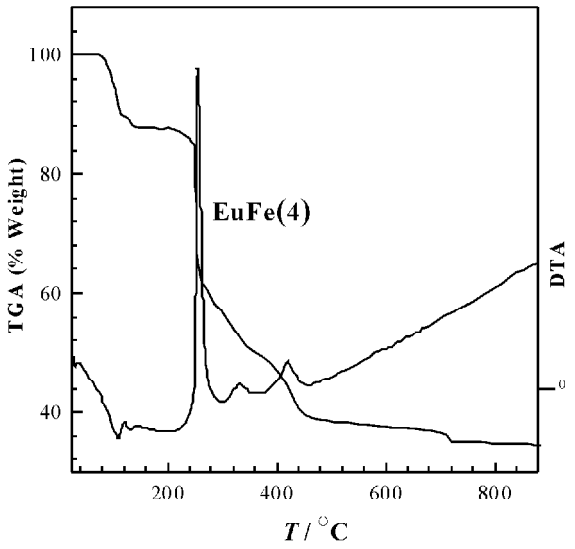

Fig. 1. Thermal analysis curves (TG and DTA) of [Eu^{III}(18-crown-6)$(H_2O)_3$][$Fe^{III}(CN)_6$]·$2H_2O$ (**4**) in nitrogen atmosphere. Heating rate: 2°C min^{-1}. Weight of the sample: 12.24 mg.

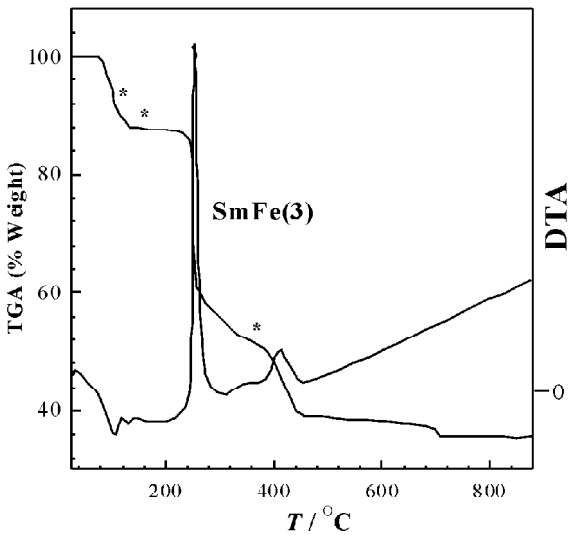

Fig. 3. Thermal analysis curves (TG and DTA) of [Sm^{III}(18-crown-6)$(H_2O)_3$][$Fe^{III}(CN)_6$]·$2H_2O$ (**3**) in nitrogen atmosphere. Heating rate: 2°C min^{-1}. Weight of the sample: 10.42 mg.

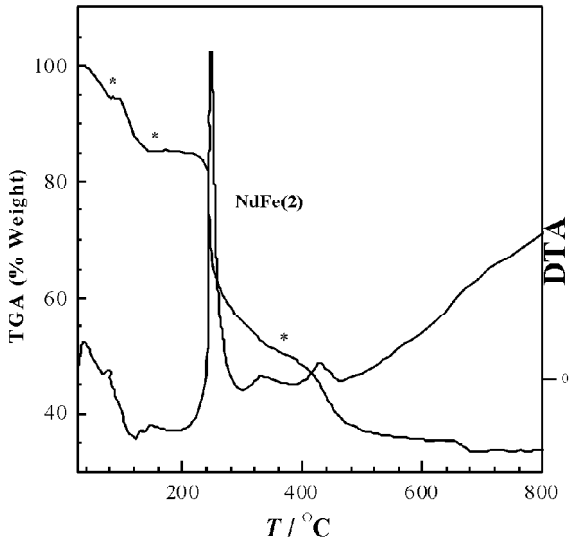

Fig. 2. Thermal analysis curves (TG and DTA) of [Nd^{III}(18-crown-6)$(H_2O)_4$][$Fe^{III}(CN)_6$]·$2H_2O$ (**2**) in nitrogen atmosphere. Heating rate: 2°C min^{-1}. Weight of the sample: 11.39 mg.

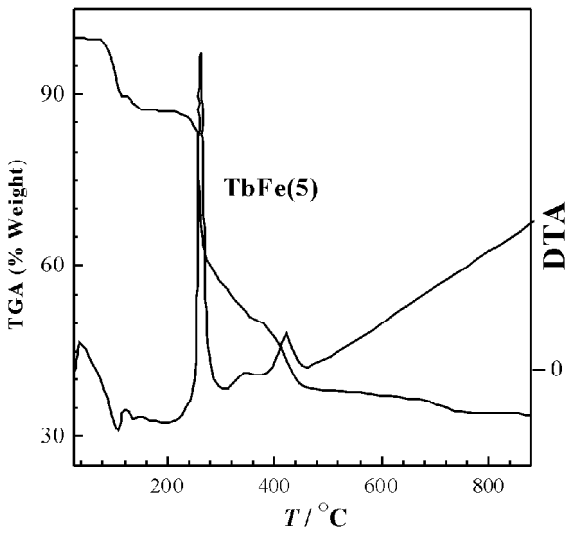

Fig. 4. Thermal analysis curves (TG and DTA) of [Tb^{III}(18-crown-6)$(H_2O)_3$][$Fe^{III}(CN)_6$]·$2H_2O$ (**5**) in nitrogen atmosphere. Heating rate: 2°C min^{-1}. Weight of the sample: 9.88 mg.

$2H_2O$ (**1**-**8**) have been carried out over the temperature 25°C to 900°C. Figs. 1 and 2 show the typical TG and DTA characteristics of [Eu^{III}(18-crown-6)$(H_2O)_3$][$Fe^{III}(CN)_6$]·$2H_2O$ (**4**) and [Nd^{III}(18-crown-6)$(H_2O)_4$][$Fe^{III}(CN)_6$]·$2H_2O$ (**2**), while the TG and DTA curves of other compounds are shown in Figs. 3–8. The thermal decomposition of all the compounds is summarized in Tables 1 and 2. Elemental analyses (%) and FT-IR data (cm^{-1}) of the selected intermediates are summarized in Tables 3 and 4, respectively.

As illustrated in Fig. 1, thermal decomposition of [Eu^{III}(18-crown-6)$(H_2O)_3$][$Fe^{III}(CN)_6$]·$2H_2O$ (**4**) takes place in six steps. The first step involves the loss of four water molecules be-

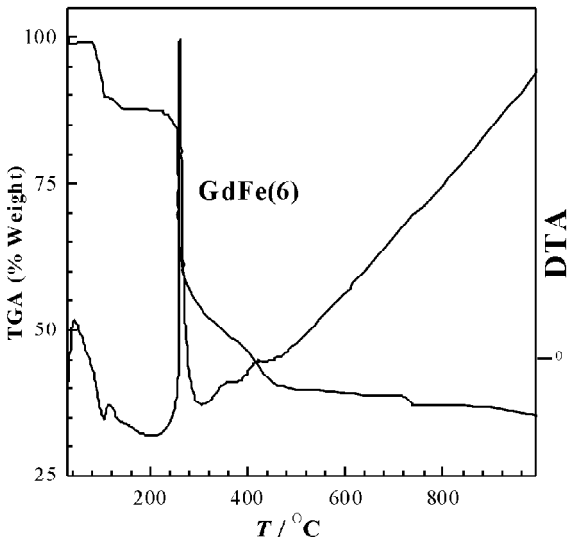

Fig. 5. Thermal analysis curves (TG and DTA) of $[Gd^{III}(18\text{-crown-}6)(H_2O)_3][Fe^{III}(CN)_6]\cdot 2H_2O$ (**6**) in nitrogen atmosphere. Heating rate: 2°C min^{-1}. Weight of the sample: 10.75 mg.

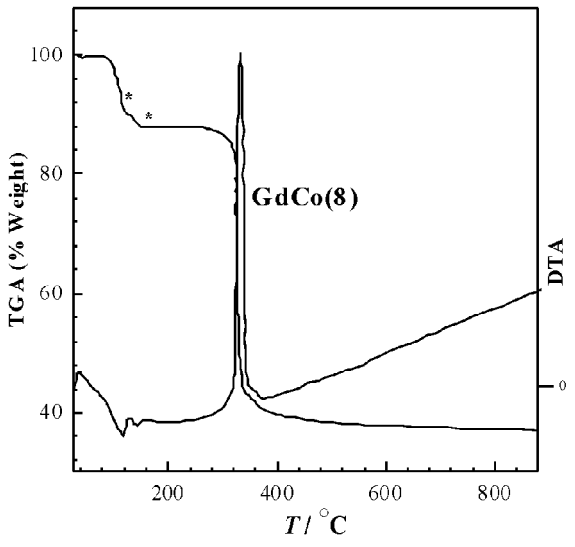

Fig. 7. Thermal analysis curves (TG and DTA) of $[Gd^{III}(18\text{-crown-}6)(H_2O)_3][Co^{III}(CN)_6]\cdot 2H_2O$ (**8**) in nitrogen atmosphere. Heating rate: 2°C min^{-1}. Weight of the sample: 10.58 mg.

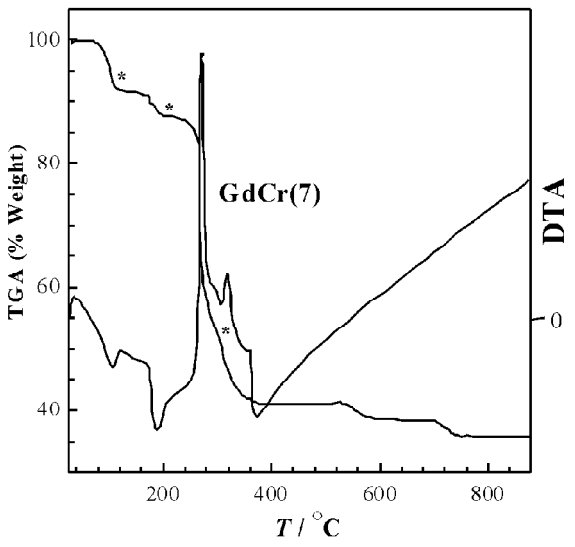

Fig. 6. Thermal analysis curves (TG and DTA) of $[Gd^{III}(18\text{-crown-}6)(H_2O)_3][Cr^{III}(CN)_6]\cdot 2H_2O$ (**7**) in nitrogen atmosphere. Heating rate: 2°C min^{-1}. Weight of the sample: 12.14 mg.

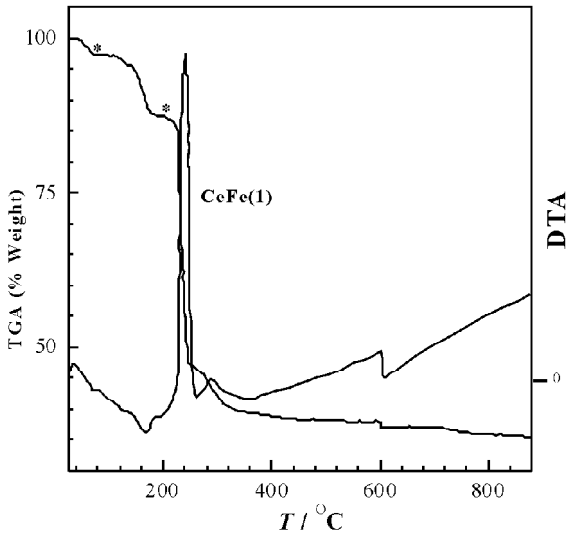

Fig. 8. Thermal analysis curves (TG and DTA) of $[Ce^{III}(18\text{-crown-}6)(H_2O)_4][Fe^{III}(CN)_6]\cdot 2H_2O$ (**1**) in nitrogen atmosphere. Heating rate: 2°C min^{-1}. Weight of the sample: 11.92 mg.

tween 73°C and 125°C, of which two are coordinated water molecules. The observed weight loss (9.8%) is in good agreement with the calculated value (10.02%). In the second step, the loss of the remaining water molecule (observed weight loss 2.53%, calcd. 2.50%) takes place in the temperature range 120–144°C. Both the dehydration steps are endothermic. In the third (221–299°C) and forth (299–358°C) steps, vigorous exothermic reactions occur due to the burning of crown ether molecule. The observed weight loss at this stage (37.25%) is fairly matching with the calculated value (36.79%), indicating the formation of $EuFe(CN)_6$. Further oxidation of this material takes place between 366°C and 458°C (fifth step;

Table 1. Thermogravimetric data of the $Ce^{III}Fe^{III}$ (**1**), $Nd^{III}Fe^{III}$ (**2**), $Sm^{III}Fe^{III}$ (**3**) and $Eu^{III}Fe^{III}$ (**4**) compounds

Step	$Ce^{III}Fe^{III}$ (**1**)	$Nd^{III}Fe^{III}$ (**2**)	$Sm^{III}Fe^{III}$ (**3**)	$Eu^{III}Fe^{III}$ (**4**)
1	38–76°C, 2.79% (calcd. for $1H_2O$, 2.48%)	40–80°C, 5.46% (calcd. for $2H_2O$, 4.94%)	73–115°C, 9.78% (calcd. for $4H_2O$, 10.04%)	73–120°C, 9.8% (calcd. for $4H_2O$, 10.02%)
2	109–185°C, 10.09% (calcd. for $5H_2O$, 12.42%)	95–145°C, 9.32% (calcd. for $4H_2O$, 9.88%)	120–148°C, 2.39% (calcd. for $1H_2O$, 2.51%)	120–144°C, 2.53% (calcd. for $1H_2O$, 2.50%)
3	196–262°C, 40.36%	225–310°C, 30.18%	218–305°C, 31.39%	221–299°C, 30.63%
4	262–348°C, 8.79%	310–370°C, 4.78%	305–373°C, 4.77%	299–358°C, 6.62%
5	358–608°C, 2.25%	370–610°C, 14.88%	377–454°C, 13.04%	366–458°C, 12.71%
6		658–680°C, 1.73%	675–724°C, 2.99%	688–736°C, 2.93%
1 + 2	12.88% (calcd. for $6H_2O$, 14.91%)	14.78% (calcd. for $6H_2O$, 14.82%)	12.17% (calcd. for $5H_2O$, 12.55%)	12.33% (calcd. for $5H_2O$, 12.52%)
3 + 4		34.96% (calcd. for crown, 36.28%)	36.16% (calcd. for crown, 36.88%)	37.25% (calcd. for crown, 36.79%)
5 + 6		16.61% (calcd. for $NdFe(CN)_6$ to $NdFeO_3$, 14.83%)	16.03% (calcd. for $SmFe(CN)_6$ to $SmFeO_3$, 15.08%)	15.64% (calcd. for $EuFe(CN)_6$ to $EuFeO_3$, 15.05%)
3 + 4 + 5	51.4% (calcd. for [Ce(crown)] $[Fe(CN)_6$ to $CeFeO_{3.5}$, 50.30%)			
Total	64.28% (calcd. 65.21%)	66.35% (calcd. 65.93%)	64.36% (calcd. 64.51%)	65.22% (calcd. 64.36%)

Table 2. Thermogravimetric data of the $Tb^{III}Fe^{III}$ (**5**), $Gd^{III}Fe^{III}$ (**6**), $Gd^{III}Cr^{III}$ (**7**) and $Gd^{III}Co^{III}$ (**8**) compounds

Step	$Tb^{III}Fe^{III}$ (**5**)	$Gd^{III}Fe^{III}$ (**6**)	$Gd^{III}Cr^{III}$ (**7**)	$Gd^{III}Co^{III}$ (**8**)
1	74–120°C, 9.9% (calcd. for $4H_2O$, 9.93%)	75–111°C, 9.31% (calcd. for $4H_2O$, 9.95%)	70–120°C, 8.52% (calcd. for $4H_2O$, 10.00%)	79–127°C, 9.62% (calcd. for $4H_2O$, 9.90%)
2	124–151°C, 2.79% (calcd. for $1H_2O$, 2.48%)	113–144°C, 2.18% (calcd. for $1H_2O$, 2.48%)	166–208°C, 3.8% (calcd. for $1H_2O$, 2.50%)	129–156°C, 2.13% (calcd. for $1H_2O$, 2.47%)
3	213–296°C, 29.78%	215–302°C, 33.99%	222–306°C, 37.27% (calcd. for crown, 36.72%)	270–374°C, 50.53% (calcd. for [Gd(crown)] $Co(CN)_6$ to $GdCoO_3$, 51.26%)
4	296–367°C, 6.8%.	302–368°C, 4.85%		
5	375–460°C, 13.14%	378–448°C, 9.72%	306–333°C, 7.1%	
6	670–750°C, 3.16%	716–744°C, 3.1%	333–372°C, 1.84%	
7			530–593°C, 2.81%	
8			696–751°C, 2.60%	
1 + 2	12.69% (calcd. for $5H_2O$, 12.41%)	11.49% (calcd. for $5H_2O$, 12.43%)	12.32% (calcd. for $5H_2O$, 12.50%)	11.75% (calcd. for $5H_2O$, 12.37%)
3 + 4	36.58% (calcd. for crown, 36.44%)	38.84% (calcd. for crown, 36.52%)		
5 + 6	16.30% (calcd. for $TbFe(CN)_6$ to $TbFeO_3$, 14.91%)	12.82% (calcd. for $GdFe(CN)_6$ to $GdFeO_3$, 14.94%)		
5 + 6 + 7 + 8			14.35% (calcd. for $GdCr(CN)_6$ to $GdCrO_3$ 15.02%)	
Total	65.57% (calcd. 63.76%)	63.15% (calcd. 63.89%)	63.94% (calcd. 64.24%)	62.28% (calcd. 63.63%)

12.71%) and at *ca*. 700°C (sixth step; 2.93%). The weight loss (15.64%) in these last two steps agrees well with the conversion of $EuFe(CN)_6$ to $EuFeO_3$ (calcd. 15.05%). Presumably, the product obtained in the fifth step is a mixture of

Table 3. Elemental analysis data (%) of the intermediates formed during dissociation of **1**, **2**, **3**, **7** and **8**

Compd.		Step 1		Step 2		Step 3		Step 4	
		Calcd.	Found	Calcd.	Found	Calcd.	Found	Calcd.	Found
1	C	30.60	30.18	35.07	35.40				
	H	4.85	4.94	3.92	3.99				
	N	11.90	11.76	13.63	13.51				
2	C	31.22	31.40	34.84	34.60			20.23	19.95
	H	4.66	4.74	3.90	3.82			0.00	0.02
	N	12.13	12.25	13.54	13.61			23.59	23.40
3	C	33.54	33.28	34.50	34.78			19.89	19.63
	H	4.06	4.15	3.86	3.77			0.00	0.03
	N	13.04	12.90	13.41	13.55			23.19	22.90
7	C	33.38	33.12	34.33	34.45	19.72	19.97		
	H	4.05	4.15	3.84	3.89	0.00	0.02		
	N	12.97	12.90	13.35	13.47	23.00	23.21		
8	C	33.03	33.29	33.96	33.74				
	H	4.00	3.91	3.80	3.73				
	N	12.84	12.97	13.20	13.36				

Table 4. FT-IR spectral data (cm^{-1}) of the intermediates formed during dissociation

Compd.	Composition	$\nu_{C=N}$	ν_{C-O}	ν_{O-H}
1	$[Ce^{III}(18\text{-crown-6})(H_2O)_4][Fe^{III}(CN)_6]\cdot 2H_2O$	2127m, 2112m	1081s	3333m, 3159br
	$[Ce^{III}(18\text{-crown-6})(H_2O)_4][Fe^{III}(CN)_6]\cdot H_2O$	2127m, 2112m	1082s	3331m, 3159br
	$[Ce^{III}(18\text{-crown-6})][Fe^{III}(CN)_6]$	2122m	1080w	–
2	$[Nd^{III}(18\text{-crown-6})(H_2O)_4][Fe^{III}(CN)_6]\cdot 2H_2O$	2129m, 2114m	1071s	3397br, 3164m
	$[Nd^{III}(18\text{-crown-6})(H_2O)_4][Fe^{III}(CN)_6]$	2125m	1071s	3407m
	$[Nd^{III}(18\text{-crown-6})][Fe^{III}(CN)_6]$	2121m	1075w	–
	$Nd^{III}Fe^{III}(CN)_6$	2136s		–
3	$[Sm^{III}(18\text{-crown-6})(H_2O)_3][Fe^{III}(CN)_6]\cdot 2H_2O$	2131m, 2117m	1073s	3346br, 2961m
	$[Sm^{III}(18\text{-crown-6})(H_2O)][Fe^{III}(CN)_6]$	2132m, 2119m	1075s	3391br
	$[Sm^{III}(18\text{-crown-6})][Fe^{III}(CN)_6]$	2124m	1076w	–
	$Sm^{III}Fe^{III}(CN)_6$	2141s	–	–
7	$[Gd^{III}(18\text{-crown-6})(H_2O)_3][Cr^{III}(CN)_6]\cdot 2H_2O$	2152m, 2125m	1073s	3349br, 2962m
	$[Gd^{III}(18\text{-crown-6})(H_2O)][Cr^{III}(CN)_6]$	2154m, 2126m	1073s	3393br
	$[Gd^{III}(18\text{-crown-6})][Cr^{III}(CN)_6]$	2140m	1076w	–
	$Gd^{III}Cr^{III}(CN)_6$	2155s	–	–
8	$[Gd^{III}(18\text{-crown-6})(H_2O)_3][Co^{III}(CN)_6]\cdot 2H_2O$	2150m, 2123m	1073s	3350br, 2959m
	$[Gd^{III}(18\text{-crown-6})(H_2O)][Co^{III}(CN)_6]$	2151m, 2123m	1074s	3390br
	$[Gd^{III}(18\text{-crown-6})][Co^{III}(CN)_6]$	2138m	1074w	–

Table 5. The exothermic pick temperatures obtained from DTA at the fast decomposition step of the compounds, **1**-**8**

Ln	CeFe (**1**)	NdFe (**2**)	SmFe (**3**)	EuFe (**4**)	TbFe (**5**)	GdFe (**6**)	GdCr (**7**)	GdCo (**8**)
T_d (°C)	241	249	254	256	263	256	270	332

Eu_2O_3, Fe_2O_3 and some carbon, which at *ca.* 700°C becomes $EuFeO_3$ (Eu_2O_3 and Fe_2O_3). The total weight loss from the initial to the final state is 65.22%, which is in good agreement with the expected value (64.36%).

The thermal behavior (Figs. 3–5; Tables 1 and 2) of **3** (SmFe), **5** (TbFe) and **6** (GdFe) are very similar to that of **4** (EuFe). In contrast, although the nature of the final product is similar for **7** (GdCr) and **8** (GdCo) (Figs. 6 and 7; Table 2), the stepwise decomposition is slightly different in these two cases. In case of **7** (GdCr), the burning of the crown ether moiety takes place in a single step and the conversion of $GdCr(CN)_6$ to $GdCrO_3$ is occurred in four steps (Fig. 6; Table 2). For compound **8** (GdCo), $[Gd(18\text{-crown-6})][Co(CN)_6]$ species is converted to the final product, $GdCoO_3$, in a single step (Fig. 7; Table 2).

Except the removal of the water molecules, the decomposition of the compound **2** (NdFe) (Fig. 2; Table 1) is similar to that of **3** (SmFe), **4** (EuFe), **5** (TbFe) and **6** (GdFe). In this case, two water molecules of crystallization are removed (obsd. weight loss, 5.46%; calcd. 4.94%) in the first step (40–80°C) and the four coordinated water molecules are removed (obsd. weight loss, 9.32%; calcd. 9.88%) in the second step (95–145°C). For the CeFe compound (**1**) (Fig. 8; Table 1), the expected final product should contain CeO_2. In this case, although the total observed weight loss (64.28%) is in good agreement with the calculated value (65.21%) for the conversion of $[Ce^{III}(18\text{-crown-6})(H_2O)_4][Fe^{III}(CN)_6]\cdot 2H_2O$ to $CeFeO_{3.5}$, it has not been possible to get matching in the individual steps.

Thermal decomposition mechanism of the compounds:

Based on the TG analyses mentioned above, thermal decomposition mechanisms of the titled compounds are shown in Scheme 1.

The first two steps are the dehydration processes in which a total of five (for **3**-**8**) or six (for **1** and **2**) coordinated and solvated water molecules are lost. The decomposition processes of dehydrated compounds can be divided into three

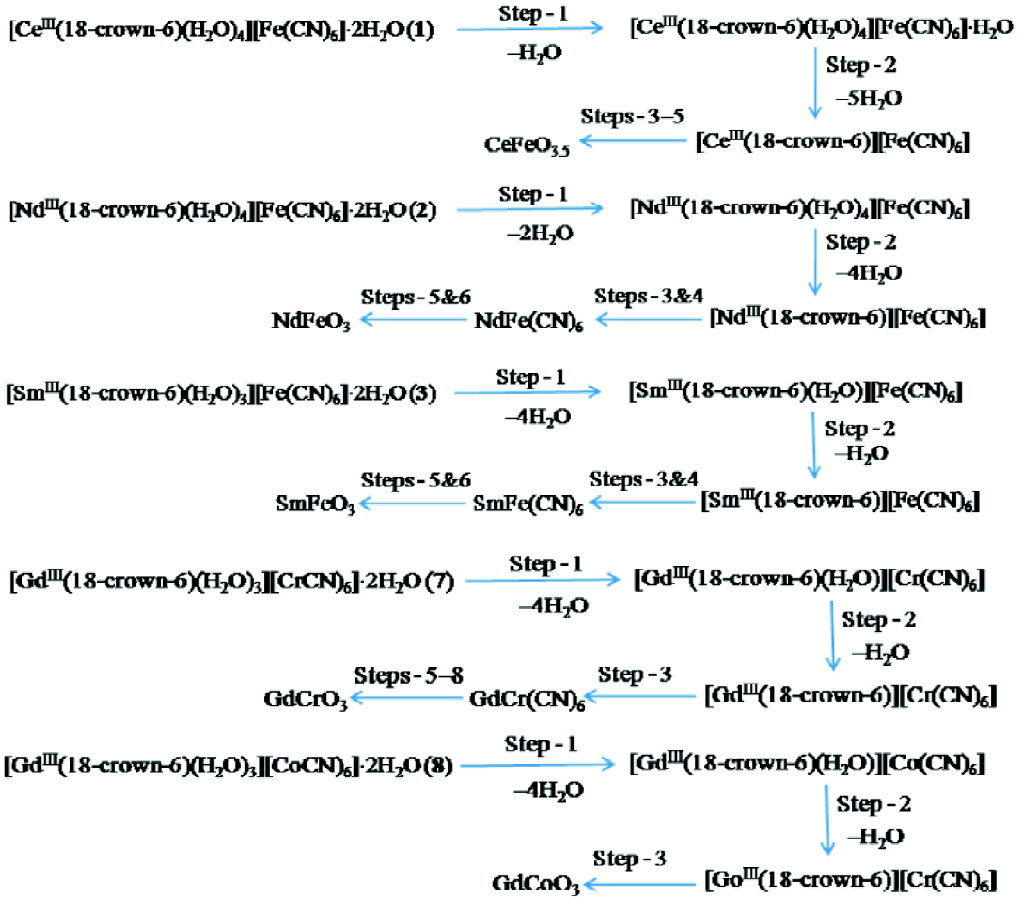

Scheme 1. Proposed thermal decomposition mechanism of the compounds **1**-**3**, **7** and **8**.

classes: (i) compounds **1** (CeFe) and **8** (GdCo) decompose in almost similar fashion, except that **1** decomposes in three steps whereas **8** decomposes in a single step; (ii) NdFe (**2**), SmFe (**3**), TbFe (**5**) and GdFe (**6**) compounds decompose to $[Ln^{III}M^{III}(CN)_6]$ in two steps then to $Ln^{III}M^{III}O_3$ in two steps; (iii) in the case of GdCr (**7**) compound, decomposition to $[Gd^{III}Cr^{III}(CN)_6]$ takes place in a single step and finally to $Ln^{III}M^{III}O_3$ in four steps.

In order to support the decomposition mechanism mentioned above, we have isolated and identified some intermediates (corresponding to compounds formed at various points, marked asterisks (*), of the DTA curves in Figs. 2, 3, 6–8) formed during the thermal decomposition of CeFe (**1**), NdFe (**2**), SmFe (**3**), GdCr (**7**) and GdCo (**8**) compounds, using elemental analyses and FT-IR spectra. The results are listed in Tables 3 and 4, revealing that the elemental analyses and FT-IR spectral data corroborate the compositions of the intermediates based on TG-DTA.

It can also be seen in Table 5 that the first decomposition peak temperature, T_d, of all the $Ln^{III}Fe^{III}$ compounds are above 256°C and this value increases, except for GdFe compound (**6**), regularly with increasing atomic number of the lanthanides. Hence, their thermal stability with respect to the decomposition of crown ether moiety increases accordingly. As evidenced from Table 4, the order of thermal stability with respect to the decomposition of crown ether moiety for the three $Gd^{III}M^{III}$ compounds is GdCo > GdCr > GdFe.

Conclusions

TG-DTA, elemental analyses and FT-IR spectra have been jointly utilized to conclude the mechanisms of thermal decomposition of a series of crown ether based lanthanide(III) hexacyanometallate compounds. The relative thermal stability of the systems has also been addressed. It has been found that the thermal stability of $Ln^{III}Fe^{III}$ compounds (Ln = Ce, Nd, Sm, Eu and Tb; except Gd) with respect to the decomposition of the crown ether moiety increases with increasing atomic number of the lanthanides and the order of this type of stability for the three $Gd^{III}M^{III}$ compounds is GdCo > GdCr > GdFe. The compounds are finally converted to the corresponding 3d-4f oxides. The present study is among only limited examples of thermal degradation of crown ether based lanthanide compounds.

Acknowledgements

RK thanks Bhairab Ganguly College for providing computer and internet facility to prepare the manuscript and carrying out FR-IR (RUSA 2.0 Challenge Level Funding) spectral study. RK gratefully acknowledged National Higher Education Mission, Ministry of Human Resource Development, Govt. of India for RUSA 2.0 fund. Financial support from Department of Science and Technology, Government of India (INSPIRE Fellowship to SM) is also gratefully acknowledged.

References

1. (a) M. E. Brown, "Introduction to Thermal Analysis Techniques and Applications", Kluwer Academic Publishers, 2004; (b) M. Feist, *ChemTexts*, 2015, **1**, 8.
2. (a) A. K. Jha, *J. Indian Chem. Soc*., 2018, **95**, 35; (b) A. Chattopadhyay, *J. Indian Chem. Soc*., 2014, **91**, 425; (c) S. Malik and S. Wankhede, *J. Indian Chem. Soc*., 2014, **91**, 2173.
3. R. F. de Farias, C. Airoldi and H. Scatena (Jr.), *Polyhedron*, 2002, **21**, 1677.
4. (a) J. D. J. Backer-Dirks, J. E. Cooke, A. M. R. Galas, J. S. Ghotra, C. J. Gray, F. Alan Hart and M. B. Hursthouse, *J. Chem. Soc*., *Dalton Trans*., 1980, 2191; (b) K. Mohanan and M. Thankamony, *J. Indian Chem. Soc*., 2012, **89**, 155.
5. (a) C.-M. Yin, Z.-R. Liu, Y.-H. Kong, C.-Y. Wu, D.-H. Ren, Y.-G. Lii and H.-F. Xue, *Thermochimica Acta*, 1992, **204**, 251; (b) M. F. Belian, S. Alves (Jr.), Gilberto F. de Sá, W. E. Silva and R. F. de Farias, *Thermochimica Acta*, 2005, **437**, 59.
6. (a) M. C. F. C. Felinto, C. S. Tomiyama, H. F. Brito, E. E. S. Teotonio and O. L. Maltac, *J. Solid State Chem*., 2003, **171**, 189; (b) C. M. Yin, Y. H. Kong, Z. R. Liu, C. Y. Wu, D. H. Ren, M. A. He and H. F. Xue, *J. Therm. Anal*., 1989, **35**, 2471; (c) J.-C. G. Biinzli and D. Wessner, *Helvetica Chimica Acta*, 1981, **64**, 582.
7. P. Misra, R. Koner, M. Nayak, S. Mohanta, J. N. Low, G. Ferguson and C. Glidewell, *Acta Cryst*., 2007, **C63**, m440.
8. R. Koner, M. Nayak, G. Ferguson, J. N. Low, C. Glidewell, P. Misra and S. Mohanta, *CrystEngComm*, 2005, **7**, 129.